Chemosphere 333 (2023) 138940

Contents lists available at ScienceDirect

Chemosphere

journal homepage: www.elsevier.com/locate/chemosphere

Characterization of chemical components of fresh and aged aerosol from vehicle exhaust emissions in Hong Kong

Ka Hei Lui [a], Yik-Sze Lau [a,b], Hon Yin Poon [c], Bruce Organ [d], Man-Nin Chan [c], Hai Guo [e], Steven Sai Hang Ho [f,g], K.F. Ho [a,*]

[a] The Jockey Club School of Public Health and Primary Care, The Chinese University of Hong Kong, Hong Kong, China
[b] International Laboratory of Air Quality and Health (ILAQR), Queensland University of Technology, Australia
[c] Earth System Science Programme, The Chinese University of Hong Kong, Hong Kong
[d] Jockey Club Heavy Vehicle Emissions Testing and Research Centre, Hong Kong, China
[e] Department of Civil and Structural Engineering, The Hong Kong Polytechnic University, Hong Kong
[f] Division of Atmosphere Sciences, Desert Research Institute, Reno, NV, 89512, United States
[g] Hong Kong Premium Services and Research Laboratory, Cheung Sha Wan, Kowloon, Hong Kong, China

HIGHLIGHTS

- Pyrene and succinic acid dominate in total fresh and aged emission respectively.
- Euro 3 vehicles pose highest fresh emission for all n-alkane compounds.
- Phthalic acid is most abundant EF_{fresh} component in aromatic acid group compounds.
- High A/F ratios (>200) in diacid compounds show intense photochemical aging process.
- Strong correlation between acid species and toluene implies possible photooxidation.

GRAPHICAL ABSTRACT

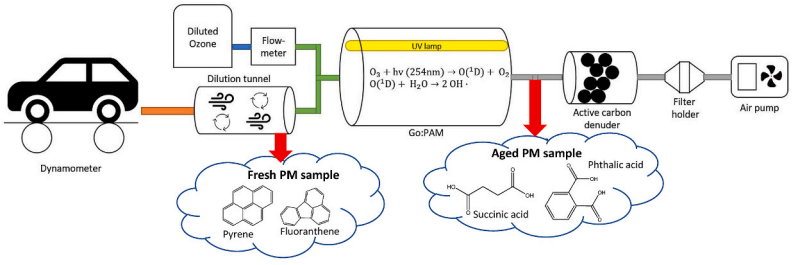

ARTICLE INFO

Handling Editor: Volker Matthias

Keywords:
Secondary organic aerosol
Chemical components
Atmospheric aging
Vehicular exhaust aerosols
Photochemistry

ABSTRACT

The chemical properties of fresh and aged aerosol emitted during controlled vehicular exhaust emissions were characterized in the analysis. Pyrene (10417.1 ± 534.9 ng kg^{-1}) is the most abundant of all analyzed compounds in total fresh emission and succinic acid (57359.8 ± 4000.3 ng kg^{-1}) is for the total aged emission. The fresh emission factors (EF_{fresh}) of all compounds in the n-alkanes group demonstrate higher average emissions for the two vehicles with EURO 3 standard compared to the other vehicles. The EF_{fresh} for benzo [*a*]pyrene is in descending order: G1 (183.1 ± 144.7 ng kg^{-1}) > G3 (103.4 ± 60.1 ng kg^{-1}) > G4 (91.2 ± 80.1 ng kg^{-1}) > G2 (88.6 ± 93.9 ng kg^{-1}). Aged/fresh (A/F) emission ratios (>20) confirmed that these diacid compounds are generated by the photooxidation of primary pollutants that emitted from gasoline combustions. High A/F ratios (>200) in phthalic acid, isophthalic acid and terephthalic acid under idling mode imply relatively more intense photochemical reactions for their productions compared with other chemical groups. Strong positive correlations ($r > 0.6$) were observed between the degradation of toluene and formations of pinonic acid, succinic acid, adipic acid, terephthalic acid, glutaric acid and citramalic acid after the aging process, suggesting possible photooxidation of toluene that can lead to secondary organic aerosol (SOA) formation in the urban atmosphere. The

* Corresponding author.
E-mail addresses: kaheilui@cuhk.edu.hk (K.H. Lui), kfho@cuhk.edu.hk (K.F. Ho).

https://doi.org/10.1016/j.chemosphere.2023.138940
Received 10 February 2023; Received in revised form 11 April 2023; Accepted 12 May 2023
Available online 16 May 2023

findings demonstrate that vehicle emission standards for pollution in relation to the change of particulate matter chemical compositions and SOA formations. The results warrant a need for regulated reformulation for such vehicles.

1. Introduction

The chemical characterization of vehicular aerosol particles is an important topic in atmospheric science. Vehicle exhaust emissions have attracted much attention due to their role as an important source of atmospheric particulate matter (PM) in urban areas with significant impacts on global climate, air quality, and human health (Nesamani, 2010; Pey et al., 2009; Sánchez-Ccoyllo et al., 2009). Organic aerosol (OA) consists of primary organic aerosols (POA) that can either be directly emitted from biogenic and anthropogenic sources (e.g., fossil fuel combustion, biomass burning, and industrial processes) or formed as secondary organic aerosols (SOA) through the reactions with volatile organic compounds (VOCs), intermediate volatility organic compounds (IVOCs) and semi-volatile organic compounds (SVOCs). These reactions can occur in the presence of oxidants (e.g., hydroxyl radical (•OH), ozone (O_3) and nitrate radical ($•NO_3$)) and further undergo the condensed phase partition (Bond et al., 2004; Jimenez et al., 2009). Secondary organic aerosol is a large fraction of the submicron aerosol and an important indicator to elucidate the impacts of aerosols related to health, climate, and visibility (Baltensperger et al., 2008; Pope et al., 2006; Stocker et al., 2013; WENT, 1960; Zhang et al., 2007). Past studies used various instruments to demonstrate that SOA production typically exceeds the direct particulate matter emissions no less than 1 h after photo-oxidation in daytime conditions (Gordon et al., 2014; Nordin et al., 2013; Platt et al., 2013; Zhao et al., 2017).

The chemical composition and yield of particulate emissions from vehicles depend on numerous factors, such as engine type, exhaust after-treatment systems, fuel additives (e.g., lubrication oil), operation conditions (i.e., engine speed and engine load), and also environmental conditions (e.g., temperature) (Kittelson et al., 2006a; Kittelson et al., 2008; Kittelson et al., 2006b; Maricq, 2007). Previous studies showed that gasoline-fueled vehicles can potentially be a major source of SOA in the United States (US) (Gentner et al., 2017; Hayes et al., 2015; Morino et al., 2022; Tkacik et al., 2014; Zhao et al., 2018). Vehicles equipped with gasoline direct injection (GDI) engines have reached ~55.3% market share in the US since 2020 and become increasingly popular worldwide (Davis et al., 2015; U.S. Department of Energy, Office of Energy Efficiency & Renewable Energy, Vehicle Technologies Office, 2021). According to Hong Kong Transport Department, gasoline-fueled vehicles contributed about 94% of all licensed private cars in 2021 (Hong Kong Transport Department, 2021). The market share of gasoline vehicles equipped with direct injection (DI) systems is steadily increasing due to better fuel efficiency and consequently lower carbon dioxide (CO_2) emissions than in conventional port fuel injection (PFI) engines (Alkidas and Management, 2007; Liang et al., 2013; Myung et al., 2012). A past study reaffirmed that GDI vehicles can potentially enhance SOA formation against port fuel injection (PFI) vehicles (Zimmerman et al., 2016). A previous study found that traffic emissions dominated wintertime SOA production potentials at a near-highway site in North Carolina (Saha et al., 2018). A study reported SOA formation from in-use vehicle emissions from highway tunnel in the US and identified that photo-oxidation can generate a substantial amount of ammonium nitrate that often exceed the mass of SOA (Tkacik et al., 2014). A study estimated that unspeciated cyclic compounds are the dominant components of gasoline-exhaust intermediate-volatility organic compounds (Lu et al., 2018).

Several studies have demonstrated that vehicle exhaust is a primary source of dicarboxylic acid (diacid) emissions (Fraser et al., 1998; Kawamura and Kaplan, 1987; Wentzell et al., 2013). A past study investigated molecular distributions of monocarboxylic acids (carbon numbers of 1–10) in the motor exhaust and identified internal combustion engines are important primary sources of volatile organic acids in the urban atmosphere (Kawamura et al., 2000). A previous study identified n-alkanes compounds in the particulate matter emissions from non-smoking gasoline-powered motor vehicles (Schauer et al., 2008). Polycyclic aromatic hydrocarbons (PAHs) have been determined in modern diesel and gasoline engine exhaust (Alkurdi et al., 2013; Cheung et al., 2010; Herring et al., 2015; Huang et al., 2013; Muñoz et al., 2018; Zielinska et al., 2004) and identified as carcinogenic for humans (IARC, 2010).

There is currently a lack of information about chemical composition profiles for SOA production from the photochemical oxidation of gasoline vehicle exhaust emissions. This investigation focuses solely on the chemical aspects of the emissions and discussion about effects of different engine operating conditions can be referred in elsewhere. This study aims to: (1) perform the physicochemical characterization of combustion-generated particles in gasoline vehicles; (2) evaluate the effects of atmospheric aging processes on compounds from vehicular emissions; (3) investigate the relationship between VOCs and vehicular emission compounds to explore potential formation mechanisms.

2. Materials and methods

2.1. Selection of test vehicles

Four gasoline-fueled passenger cars were recruited for testing three different driving conditions denoted as idling, cruising speed of 50 km/h (steady state), and New European Driving Cycle (NEDC). The emission

Table 1
Specifications of vehicles involved in the driving tests in this study.

Vehicle ID[a]	Year of manufacture	Vehicle model	Emission standard[b]	Mileage (km)	Weight (kg)	Engine power (hp)	Engine cylinder capacity (cc)	Fuel injection technology
G1	2005	Nissan Lafesta	EURO 3	127,757	1500	137@ 5200 rpm	1997	MPII[c]
G2	2010	BMW 320i	EURO 4	66,260	1475	170@ 6700 rpm	1995	GDI[d]
G3	2004	Honda Odyssey	EURO 3	146,115	1600	158@ 5500 rpm	2354	MPII
G4	2014	BMW 116i	EURO 5	91,380	1395	134@ 4350 rpm	1598	GDI

[a] ID denotes vehicle identification in this analysis.
[b] The emission standard refers to a vehicle emission standard established on the new land-used vehicles in the European Union (EU), and European Economic Area (EEA) member states, and United Kingdom (UK), and ships in EU.
[c] MPII denotes as multipoint indirect injection.
[d] GDI denotes as gasoline direct injection.

standards for the vehicles were classified as from EURO 3 to EURO 5. In addition, these vehicles (made in Germany and Japan) are the top five sales brands in Hong Kong (Hong Kong Transport Department, 2021). The details are listed in Table 1. The reasons to choose vehicles from Euro 3 to Euro 5 emission standard in this study were due to anticipated higher emissions and formation potentials of air pollutants compared to Euro 6. All the driving tests were conducted at the Jockey Club Heavy Vehicle Emissions Testing and Research Centre (JCEC) with EURO 6 emission testing standards in Tsing Yi, Hong Kong. The schematic diagram of the experimental setup is illustrated in Fig. S1 (Supplementary Material).

2.2. Experimental setup and sample collection

All driving tests were performed on a Mustang Chassis Dynamometer with a 48" single roller. The exhaust from the testing vehicle was directed to a constant volume sampling (CVS) system for gaseous species analyses and sample collection. The tailpipe emission from the testing vehicle was first directed to the dilution tunnel of the CVS system. In the dilution tunnel, the exhaust was mixed with air after filtration to lower the gas temperature (~25 °C) and concentration for further sampling. The diluted exhaust flow was controlled by a venturi, and the real-time measurement of gaseous species, including nitrogen oxides (NO_x), carbon monoxide (CO) carbon dioxide (CO_2), and total hydrocarbons (THC), were performed near the end of the dilution tunnel. Fresh particulate matter (PM) samples were collected simultaneously by a Teflon filter ($\Phi = 47$ mm, Pall Corporation, US) and a quartz filter ($\Phi = 47$ mm, Whatman, UK) from the dilution tunnel. The flow rate of diluted exhaust was 20 L per minute for each filter. In addition, gas sample was collected by an evacuated stainless-steel 2-L canister from the CVS in each experiment for VOC analysis. The gas sample collection procedure was repeated after the oxidation of the gas sample.

A fraction of the diluted exhaust was divided from the dilution tunnel for further photooxidation reaction experiments. Stimulated atmospheric photooxidation of the chemicals in the diluted exhaust was performed in a Gothenburg Potential Aerosol Mass (Go:PAM) reactor (ultraviolet wavelength of 254 nm). More detailed descriptions of the Go:PAM reactor can be found elsewhere (Lau et al., 2021; Watne et al., 2018). In summary, the exhaust from the dilution tunnel was mixed with O_3 and zero air before entering the Go:PAM reactor. The O_3 concentration was measured by an O_3 monitor (T400; Teledyne UV Absorption O_3 Analyzer, San Diego, CA, US). The total flow rate passing the flow-tube reactor was 9 L min^{-1} and the residence time was 46.7s. A controlled gas delivery system was used for delivering mixed steam with humidified zero air and O_3 at flow rate of 4.5 L min^{1}. Another half of the flow (from the vehicle exhaust stream) was controlled by pressure difference at the outflux of the reactor which was used for filter collection (Supplementary Material: Fig. S3). The dilution factor (DF) of exhaust was defined as the volume ratio of diluted exhaust in the dilution tunnel and the raw exhaust gas from the vehicle at a certain moment of the driving cycle. The averaged DF of gasoline exhaust in the dilution tunnel during NEDC and steady-state cycles was approximately 20. The DF in the idling cycle was approximately 50. The resulting DF of exhaust in the Go:PAM reactor was two under the experimental setup. For each experiment, the ozone concentration before entering the Go:PAM reactor was set to around 3 ppm at the beginning of the driving cycle. According to the calibration result presented in Fig. S5 (Supplementary Material), the equivalent OH exposure is around 1.8×10^{12} molec cm^{-3} s, equal to around 2 weeks of atmospheric oxidation time, taking an ambient OH concentration of 1.5×10^{6} molec cm^{-3} (Mao et al., 2009). After the photooxidation in the reactor, the stream was purged through an O_3 denuder to remove oxidants and other reactive gas-phase species. The aged gas as then split into two streams with identical flow rates (4.5 L min^{1}) using separation pumps. One stream of the aged aerosol sample was collected by a Teflon membrane filter while the other stream of the sample was collected by a quartz filter. For each vehicle, the emission tests under three driving conditions (i.e., idling, steady state, and NEDC) were conducted for the analysis. Each set of emission experiments was repeated in triplicate analysis and to also ensure sufficient sample loadings. More information on the experimental conditions is listed in Table S1 and shown in Fig. S6 (Supplementary Material).

The calibrations of •OH and O_3 concentrations were performed before analysis using the approach adopted for sulfur dioxide (SO_2) described in (Lambe et al., 2011) and (Li et al., 2015), and the result is illustrated in Fig. S5 (Supplementary Material). The experimental conditions of the oxidation were performed according to previous studies (Li et al., 2019; Zhang et al., 2020b).

2.3. Chemical analysis

The VOCs samples collected by the canisters were analyzed by a gas chromatography/mass spectrometry (GC/MS) system. More details of the instrumental settings were described by Lyu et al. (2019). Fresh and aged PM samples collected on quartz filters were analyzed by solvent extraction-gas chromatography/mass spectrometry (SE-GC/MS) method. Details of the chemical analysis of PM samples can be referred to a previous study (Lyu et al., 2019). In summary, each PM quartz filter was divided into two fractions, one half was extracted with hexane: dichloromethane (1:1), and another half was extracted with methanol. Both of the filters were sonicated and then concentrated to 1 ml using a rotatory evaporator. For the non-polar fraction, the final extract was directly injected and analyzed by a GC-MS (7890 A/5975C, Agilent Technologies, Santa Clara, CA). For polar fraction, the initial extract was further dried with a gentle flow of high-purity nitrogen gas (99.99%, Specialty Gas Engineering Company Limited, Hong Kong, China). A 20 μl of *N,O-bis*(trimethylsilyl) trifluoroacetamide (BSTFA) in 1% trimethylchlorosilane (TMCS) was then added, and pyridine was used to fill up to a final volume of 100 μl. The sample solution was sealed and transferred to heat at 70 °C for 3 h. Blank filters collected from the field were also analyzed using the same procedures.

2.4. Emission factor calculation

The emission factor is defined as the emission of a chemical compound per unit mass of fuel consumed by the vehicle (Wang et al., 2019; Zhang et al., 2020a) as shown in equation (1) below.

$$EF_{\beta} = \frac{M_{\beta}}{M_{f}\mu} \times 1000 \quad (1)$$

where EF_{β} is the emission factor of the chemical compound β, M_{β} is the total mass of the chemical compound β (g), and $M_{f\mu}$ is the mass of fuel consumed (kg). The mass of the chemical compounds emitted during the sampling period was then calculated by equation (2) (Wang et al., 2019).

$$M_{\beta} = \sum_{j=1}^{t} C_{\beta j} V_{j} \quad (2)$$

where $C_{\beta j}$ is the concentration of chemical compound β at the jth second of the cycle (g m^{-3}), V_j is the volume of the airflow in the CVS at the jth second (m^3), and t is the time duration of the cycle (s).

The fuel consumption of the vehicle over the experimental period was calculated by equation (3) as follows:

$$M_{\mu} = \sum_{j=1}^{t} \left\{ \frac{[CO_2] \times N_A}{A_v} \times \frac{MW_C}{\omega_{\mu}} \div V_j \div 1000 \right\} \quad (3)$$

where $[CO_2]$ is the volumetric concentration of CO_2 measured by the analyzer (%); N_A is the number concentration of air (molecule/m^3); A_V is the Avogadro constant (molecule/mol); MW_C is the molecular weight of carbon (g/mol); ω_{μ} is the mass fraction of carbon in gasoline fuel (86%) for gasoline (Jahirul et al., 2010); V_j is the volume of the airflow in the

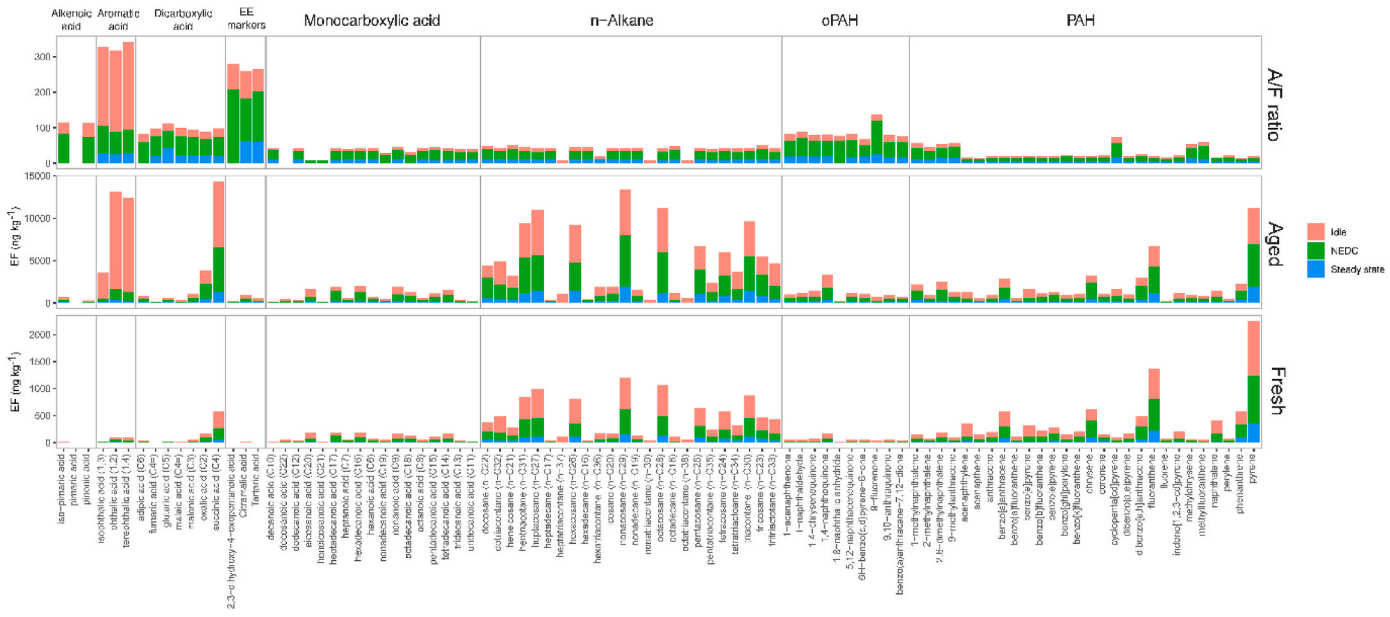

Fig. 1. Emission factors of chemical compounds in fresh and aged vehicular exhaust emission samples and corresponding aged to fresh ratios (A/F ratio) in PM under different driving conditions.

CVS at the *j*th second (m^3), and t is the time duration of the cycle (s). The emission factors of individual chemical compounds are shown in Table S2 (Supplementary Material).

2.5. Statistical analysis

Pearson'scorrelation coefficient analysis was used to test correlations between all analyzed compounds using SPSS (version 21.0, IBM, New York, NY) or GraphPad Prism (Version 5 for Windows) software.

3. Results and discussion

3.1. Emission factors for target compounds in fresh emissions

A total of 96 organic compounds in the fresh and aged aerosol samples were identified and classified into eight groups according to their chemical configurations or properties, including n-alkanes, PAHs, oxygenated-PAHs (OPAHs), alkenoic acids, aromatic acids, dicarboxylic acids, monocarboxylic acids, and motor emission markers (ME markers). The compounds consist of unique straight/branched-chain, saturated/unsaturated, or aliphatic/aromatic chemical structures. The EFs for different chemical groups in fresh emission (EF_{fresh}) and stimulated aged (EF_{aged}) are compared in Fig. 1. The results show that the chemical compositions are highly dependent on different driving conditions (Lau et al., 2023). Pyrene (10417.1 ± 534.9 ng kg^{-1}) is the most abundant chemical species in the fresh emission, while succinic acid (57359.8 ± 4000.3 ng kg^{-1}) is the top one after the aging process.

3.1.1. N-alkanes

The EF_{fresh} of the total quantified n-alkanes group is 48450.2 ± 2870.3 ng kg^{-1}, ranking the top most abundant chemical group. The EF_{fresh} for the most dominant n-alkane was nonacosane (33.2–981.1 ng kg^{-1}) which is one order of magnitude higher than the lowest one (hexadecane). Among the n-alkane homologous, some of the abundant species are with carbon numbers ranged from 24 to 27 ($C_{24\text{-}27}$), in a range of 2671.1–4543.0 ng kg^{-1}. A previous study reported the concentrations of organic compounds in fine particulate matter ($PM_{2.5}$) at the Wutong tunnel, Shenzhen, China, and found that the carbon number maximum of the n-alkanes (C_{max}) is 23 (He et al., 2006). The discrepancy of the findings could be attributed to the environments (i.e., driving test vs real traffic condition). It should be noted that gasoline-fueled vehicles showed emissions of higher carbon number of n-alkanes, additionally from lubricating oils (Schauer et al., 2002, 2008). Higher compositions of n-alkanes with medium boiling points (i.e., carbon number between 19 and 29) in the exhausts of gasoline-fueled vehicles are potentially derived from the combustion/pyrolysis and recombination of components in the fuel and lubricating oils (Schauer et al., 2002). Moreover, the EF_{fresh} for the n-alkanes group are higher in emissions from the EURO 3 than the EURO 5 standard vehicles. The phenomenon could be possibly related to the advancement emission reduction technology, but further investigation on the n-alkanes emission is required.

3.1.2. PAHs and OPAHs

The EF_{fresh} for the total quantified PAH are (72.7–1665.9 ng kg^{-1}), ranking second of the abundant chemical group in the vehicle emission tests. Pyrene is the most dominant PAHs while its EF_{fresh} is at least two orders of magnitude higher than the lowest for methylfluoranthene (2.0–48.5 ng kg^{-1}). The EF_{fresh} for the total sixteen priority PAHs defined by United States Environmental Protection Agency (U.S. Centers for Disease Control) are in a range of 242.2–6310.9 ng kg^{-1}, accounted for 83.2–84.8% of total quantified PAH. Several priority PAHs (termed Group B2) are considered probable human carcinogens, and the sum of their EF_{fresh} ranges from 77.5 to 2231.7 ng kg^{-1} with a contribution of 26.2–32.4% to the total PAHs. Benzo [*a*]pyrene (BaP) is often used as a main marker of carcinogenic PAHs (Boström et al., 2002) which can be released by various burning processes (ATSDR, 1995). The EF_{fresh} for BaP is in a descending order of G1 (183.1 ± 144.7 ng kg^{-1}) > G3 (103.4 ± 60.1 ng kg^{-1}) > G4 (91.2 ± 80.1 ng kg^{-1}) > G2 (88.6 ± 93.9 ng kg^{-1}).

This observation probably relates to incomplete combustion of fuels and lubricating oil that generate high quantity of PAHs to the PMs (Lough et al., 2007). A previous study also suggested the abundances of heavier PAHs in fuel and tailpipe emissions could be affected by engines containing aged lubricating oil (Schauer et al., 2002). Combustion-produced PAH can break out from the combustion chamber and past the piston rings with the blow-by gases that absorb in the crankcase oil (Fujita et al., 2007). The concentration levels of PAH in the lubrication oil thus elevate with mileages until the next oil change (Fujita et al., 2007). Fujita et al. (2007) further confirmed that the high-molecular-weight particulate PAHs, such as benzo (ghi)perylene, indeno (1,2,3-*cd*)pyrene, and coronene were abundant in used gasoline

motor oil, but did not present in fresh gasoline and used oil in diesel engine. The three abovementioned compounds accounted for a relatively high of ~4.7–6.4% of the total quantified PAHs, reflecting their significance in gasoline-fueled vehicle emissions.

Pyrene (72.7–1665.9 ng kg^{-1}) and fluoranthene (49.8–1123.1 ng kg^{-1}) are the two most dominant species, consistent to the observations in the examinations of non-smoking gasoline powered motor vehicles (Schauer et al., 2008). Luo et al. (2015) reported that ethanol-gasoline blended fuels could reduce soot precursors such as large n-alkanes and aromatics in different fuels (gasoline and 10% splash blended ethanol in gasoline (E10)). Our study also quantified the 16 priority PAHs and found consistent observations. Moreover, dibenz [a,h]anthracene (72.7–1665.9 ng kg^{-1}) and benzo [*a*]pyrene (72.7–1665.9 ng kg^{-1}) ranked four and nine the highest EF_{fresh}, respectively, supporting emission from light-duty gasoline-fueled vehicles are their dominant source (Miguel et al., 1998).

The EF_{fresh} for all quantified PAHs show higher in the EURO 3 than EURO 5 standard vehicles. This observation can be adequately explained by the higher combustion efficiency with advanced catalytic technology equipped with the newer version engine which could reduce the formation of incomplete combustion products. (Lin et al., 2019). A past study also found that the emissions of toxic substances are lower from the EURO 5 and 6 than EURO 3 and 4 standard vehicles (Lin et al., 2020).

For OPAHs, 1,4-naphthoquinone is the most dominant species, with the EF_{fresh} of 5.0–152.2 ng kg^{-1}, followed by 9-fluorenone (0.3–42.8 ng kg^{-1}). Zielinska et al. (2004) also found 9-fluorenone predominantly presented in emissions from different gasoline-fueled in-use vehicles (Zielinska et al., 2004).

3.1.3. Monocarboxylic acids, alkenoic acids, dicarboxylic acids, aromatic acids, and ME markers

Among the monocarboxylic acids, heptadecanoic acid has the highest EF_{fresh} (3.7–270.5 ng kg^{-1}), followed by hexadecanoic acid (4.5–162.4 ng kg^{-1}). It should be noted hexadecanoic acid is one of the dominant chemical species in the entire fresh gasoline emissions. Moreover, the high emission of hexadecanoic is consistent with the findings in the Van Nuys tunnel reported by Fraser et al. (1998). The highest EF_{fresh} in alkenoic acid group is iso-pimaric acid (0–19.4 ng kg^{-1}).

In dicarboxylic acid group, the highest EF_{fresh} is shown for succinic acid (17.6–570.9 ng kg^{-1}), followed by oxalic acid (5.9–173.5 ng kg^{-1}). The EF_{fresh} for succinic acid is ~3.5 and 75.1 times oxalic and fumaric acid (the lowest EF_{fresh}), respectively. A study specifically focuses on dicarboxylic acid emissions from a GDI engine equipped with a catalytic filter (Bock et al., 2020). The results show that oxalic acid has the highest abundance, much more than malonic acid under all conditions (Bock et al., 2020), consistent with our findings (i.e., EF_{fresh} for oxalic acid is ~2.6–4.4 times that of malonic acid under all conditions). The dicarboxylic acids could potentially form through similar mechanisms as monocarboxylic acids under the combustion event in the presence of acid precursors (e.g., aldehydes, •OH, hydrogen atoms, and opened aromatic rings), while the engine condition could significantly impact on the acid emissions (Bock et al., 2020). In this study, glutaric and adipic acid, with EF_{fresh} of 0.5–32.6 and (0–34.2 ng kg^{-1}), respectively, accounted for ~3.1 and 3.5% of total quantified dicarboxylic acids. Strong positive correlation ($r = 0.89$) was observed between these two dicarboxylic acids (Table 3), suggesting similar emission sources. Dicarboxylic acids are originated from the combustion of alkanes in fossil fuels (Kawamura and Kaplan, 1987; Rogge et al., 1993), and a previous study identified that glutaric acid and adipic acid in the vehicle emission sources are the potential sources as well (He et al., 2006).

The total EF_{fresh} for the aromatic acid group is 464.5 ± 28.0 ng kg^{-1}, while phthalic acid is the most abundant species with EF_{fresh} of 3.4–92.5 ng kg^{-1}. Our finding is consistent to Kawamura et al. (1985) which found maleic acid and phthalic acid are two major species in automobile emissions. Moreover, the diacids are probably derived from incomplete combustion products of aromatic hydrocarbons (e.g., benzene, toluene and naphthalene) in vehicular engines. Unsaturated diacids might be further oxidized to oxalic acid during the combustion process. Incomplete combustion of cyclic olefines can probably produce saturated diacid compounds in the automobile exhausts (Kawamura and Ikushima, 1993; Kawamura et al., 1985). The EF_{fresh} for the most dominant ME markers is seen for citramalic acid, with EF_{fresh} of 0.9–13.0 ng kg^{-1}.

3.2. Simulated aging processes for organic compounds in vehicle exhaust

The EF_{aged} for all quantified compounds is 10.0 ± 0.7 × 10^5 ng kg^{-1}, which is ~9.2 times the EF_{fresh} of ~1.1 ± 0.07 × 10^5 ng kg^{-1}. Fig. 1 illustrates the aged/fresh (A/F) emission ratio for all targeted individual chemical species. These species showed different oxidation properties in the stimulated photochemical aging environment and the below subsections were classified according to the impacts after the oxidations of these compounds.

3.2.1. Monocarboxylic acid, alkenoic acids, dicarboxylic acids, aromatic acids, and ME markers

The average A/F ratios for the monocarboxylic acids, alkenoic acids, dicarboxylic acids, aromatic acids, and ME markers groups are 9.3 ± 0.9, 30.9 ± 0.8, 23.3 ± 4.3, 95.5 ± 4.3 and 85.3 ± 48.6, respectively. High A/F ratios of >20 (except for docosanoic acid and pimaric acid) are observed for all diacid compounds and ME markers, potentially due to their bulks are favourite to be produced through the simulated aging processes. The diacid compounds are also oxidation products of aromatic hydrocarbons and cycloolefins (Borrás and Tortajada-Genaro, 2012; Hamilton et al., 2006). Glutaric acid and adipic acid are formed through the reactions of cycloolefins emitted from anthropogenic sources with O_3 (Hatakeyama et al., 1985).

Previous studies determined the formations of succinic acid, glutaric acid, and phthalic acid in the vehicle exhaust, showing higher rates under compression-ignition (CI) than spark-ignition (SI) vehicles. These acids are thus considered as atmospheric transformation products from CI vehicles (Chebbi and Carlier, 1996; Fraser et al., 1999; Grosjean and Seinfeld, 1989; Kawamura and Gagosian, 1987; Kawamura et al., 1996; Keywood et al., 2004a, 2004b). More investigation would be required to confirm their mechanism and transformation pathways in the future experiment.

In addition, high A/F ratios (>200) are found for three aromatic acids including phthalic acid, isophthalic acid and terephthalic acid under idling mode, suggesting relatively more intense photochemical reactions for their productions compared with other chemical groups. Phthalic acid could be generated by naphthalene or other PAHs in the atmosphere through photochemical reaction (Kawamura and Yasui, 2005), whereas the total EF_{aged} for phthalic acids is noticeably higher than the EF_{fresh} in this study. These results further support that aromatic acids could be mainly produced through secondary photochemical processes rather than direct emission from vehicular emissions.

Extremely high A/F ratios (>300) are observed for 2,3-dihydroxy-4-oxopentanoic acid under steady state, possibly ascribed to its rapid formation rate as the abovementioned compounds or decarboxylation of diacid compound (with carbon number of 4) during the aging (Zhao et al., 2018). Lau et al. (2021) identified 2,3-dihydroxy-4-oxopentanoic acid (a toluene-related SOA marker) as a product from the photooxidation reaction of toluene in a potential aerosol mass oxidation flow reactor (PAM-OFR) under OH• exposure. Moreover, succinic acid is more abundant than malonic acid originated from vehicular exhaust emissions in ambient environment (Kawamura and Kaplan, 1987; Kundu et al., 2010). Our findings (both EF_{fresh} and EF_{aged}) are consistent with the abovementioned observations. Eventually, the stimulated atmospheric aging led more formations of malonic and succinic acid (A/F ratios >20). The results confirm that these diacid compounds are generated by the photooxidation of primary pollutants that emitted from

Table 2
Individual OPAH to parent PAH ratios (±standard deviations) for different vehicular exhaust emission samples.

			Fresh[b]	Aged[c]	
Vehicle ID[a]	Parent PAH	Corresponding oxidized PAH (OPAH)	OPAH/Parent PAH ratio	OPAH/Parent PAH ratio	Aged/Fresh ratio
G1	naphthalene	1,4-naphthoquinone	0.47 ± 0.11	2.61 ± 0.57	5.61
	1-methylnaphthalene	1-naphthaldehyde	0.38 ± 0.05	0.56 ± 0.10	1.47
	fluorene	9-fluorenone	0.45 ± 0.26	2.60 ± 1.26	5.73
	anthracene	9,10-anthraquinone	0.24 ± 0.03	0.94 ± 0.16	3.87
	benzo [*a*]anthracene	benzo(*a*)anthracene-7,12-dione	0.06 ± 0.00	0.25 ± 0.04	3.96
	acenaphthylene	1-acenaphthenone	0.19 ± 0.08	1.14 ± 0.48	5.97
	acenaphthene	1-acenaphthenone	0.35 ± 0.03	1.86 ± 0.30	5.30
	chrysene	1,4-chrysenequinone	0.12 ± 0.07	0.47 ± 0.30	4.08
G2	naphthalene	1,4-naphthoquinone	0.50 ± 0.12	2.58 ± 0.59	5.14
	1-methylnaphthalene	1-naphthaldehyde	0.39 ± 0.12	0.62 ± 0.3	1.60
	fluorene	9-fluorenone	0.39 ± 0.34	2.10 ± 1.46	5.33
	anthracene	9,10-anthraquinone	0.24 ± 0.04	1.07 ± 0.29	4.52
	benzo [*a*]anthracene	benzo(*a*)anthracene-7,12-dione	0.06 ± 0.00	0.26 ± 0.02	4.43
	acenaphthylene	1-acenaphthenone	0.16 ± 0.05	0.83 ± 0.22	5.07
	acenaphthene	1-acenaphthenone	0.38 ± 0.02	2.04 ± 0.07	5.30
	chrysene	1,4-chrysenequinone	0.12 ± 0.06	0.49 ± 0.25	4.08
G3	naphthalene	1,4-naphthoquinone	0.54 ± 0.15	3.02 ± 0.56	5.61
	1-methylnaphthalene	1-naphthaldehyde	0.34 ± 0.01	0.50 ± 0.11	1.47
	fluorene	9-fluorenone	0.40 ± 0.26	2.15 ± 1.32	5.35
	anthracene	9,10-anthraquinone	0.26 ± 0.04	0.96 ± 0.14	3.76
	benzo [*a*]anthracene	benzo(*a*)anthracene-7,12-dione	0.06 ± 0.01	0.23 ± 0.03	3.76
	acenaphthylene	1-acenaphthenone	0.18 ± 0.07	0.87 ± 0.22	4.87
	acenaphthene	1-acenaphthenone	0.38 ± 0.06	1.91 ± 0.21	5.06
	chrysene	1,4-chrysenequinone	0.12 ± 0.06	0.49 ± 0.27	4.02
G4	naphthalene	1,4-naphthoquinone	0.56 ± 0.24	2.46 ± 0.64	4.39
	1-methylnaphthalene	1-naphthaldehyde	0.42 ± 0.10	0.61 ± 0.25	1.46
	fluorene	9-fluorenone	0.33 ± 0.27	1.65 ± 1.10	4.94
	anthracene	9,10-anthraquinone	0.25 ± 0.04	1.03 ± 0.36	4.11
	benzo [*a*]anthracene	benzo(*a*)anthracene-7,12-dione	0.06 ± 0.01	0.26 ± 0.07	4.25
	acenaphthylene	1-acenaphthenone	0.19 ± 0.08	0.81 ± 0.24	4.26
	acenaphthene	1-acenaphthenone	0.43 ± 0.12	1.94 ± 0.20	4.55
	chrysene	1,4-chrysenequinone	0.15 ± 0.10	0.55 ± 0.39	3.58

[a] ID denotes vehicle identification in this analysis.
[b] The emission factors for particulate matter samples as fresh (EF_{fresh}) emissions.
[c] The emission factors for particulate matter samples as aged (EF_{aged}) emissions.

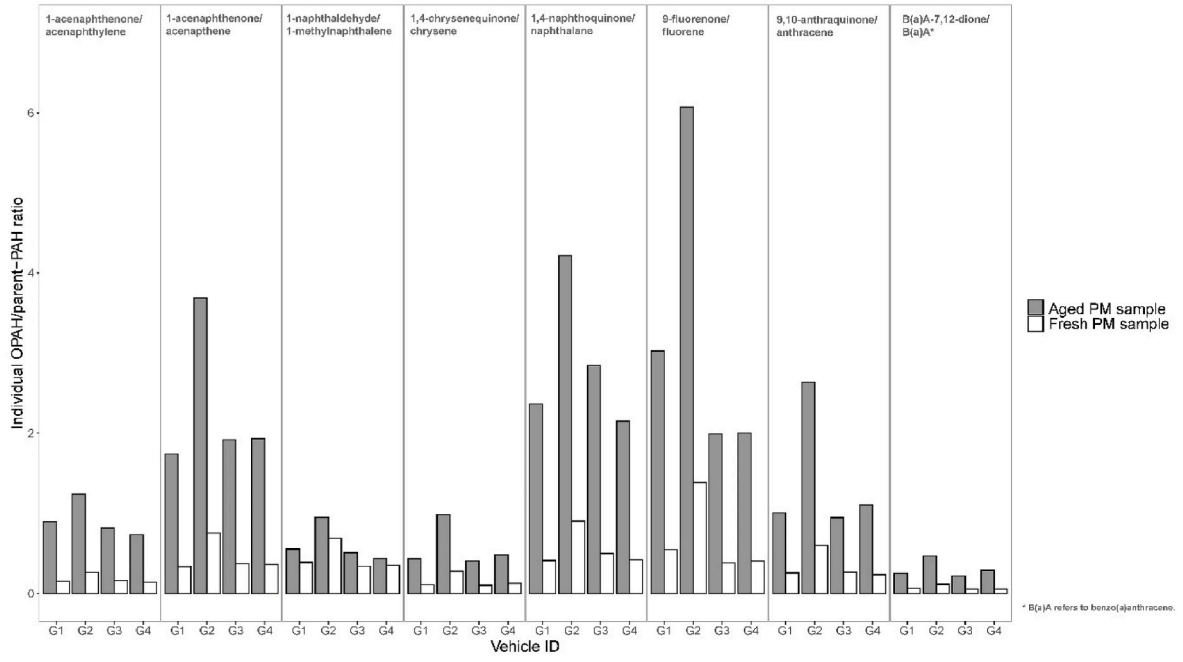

Fig. 2. Individual OPAH/parent-PAH ratio of selected compounds in fresh and aged PM samples for all tested vehicles.

gasoline combustions.

The A/F ratios for monocarboxylic acids are in a range of 7.3–11.1, implying that their secondary formations are much less than those for aromatic acids and diacids. This could be explained by relatively high volatility of low molecular weight monocarboxylic acids that are less partition in particulate phase. In addition, they are not identified as the

Table 3
Pearson's correlation coefficients (r) of volatile organic compounds degradation and formations of organic acids ($r \geq 0.60$ and 0.05 significant level).

	pinonic acid	iso-pimaric acid	pimaric acid	oxalic acid	malonic acid	maleic acid	fumaric acid	succinic acid	glutaric acid	adipic acid	phthalic acid	isophthalic acid	terephthalic acid	tartaric acid	glutaric acid	2,3-dihydroxy-4-oxopentanoic acid	citramalic acid	benzene	toluene
pinonic acid	1																		
iso-pimaric acid	0.96**[a]	1																	
pimaric acid	−0.21	−0.22	1																
oxalic acid	0.86**	0.87**	−0.52	1															
malonic acid	0.88**	0.89**	−0.55**	0.94**	1														
maleic acid	0.90**	0.96**	−0.40**	0.94**	0.94**	1													
fumaric acid	0.86**	0.91**	−0.50**	0.93**	0.92**	0.96**	1												
succinic acid	0.91**	0.82**	−0.17	0.80**	0.81**	0.77**	0.73**	1											
glutaric acid	0.80**	0.85**	−0.61**	0.92**	0.96**	0.94**	0.96**	0.72**	1										
adipic acid	0.77**	0.80**	−0.53**	0.86**	0.91**	0.86**	0.84**	0.74**	0.89**	1									
phthalic acid	0.79**	0.69**	0.04	0.53**	0.50**	0.55**	0.50**	0.70**	0.34*	0.37*	1								
isophthalic acid	0.78**	0.74**	−0.01	0.51**	0.53**	0.60**	0.56**	0.61**	0.40**	0.42**	0.95**	1							
terephthalic acid	0.77**	0.70**	0.04	0.51**	0.50**	0.56**	0.49**	0.64**	0.34*	0.38*	0.98**	0.97**	1						
tartaric acid	0.91**	0.94**	−0.2	0.87**	0.87**	0.94**	0.90**	0.83**	0.87**	0.80**	0.54**	0.57**	0.53**	1					
glutaric acid	0.96**	0.91**	−0.17	0.82**	0.82**	0.83**	0.78**	0.93**	0.72**	0.68**	0.83**	0.78**	0.80**	0.84**	1				
2,3-dihydroxy-4-oxopentanoic acid	0.70**	0.78**	−0.34*	0.83**	0.85**	0.86**	0.81**	0.68**	0.87**	0.90**	0.2	0.24	0.21	0.87**	0.60**	1			
citramalic acid	0.97**	0.96**	−0.16	0.82**	0.84**	0.89**	0.83**	0.84**	0.77**	0.71**	0.76**	0.79**	0.78**	0.90**	0.94**	0.67**	1		
benzene	−0.23	−0.1	−0.03	−0.27	−0.14	−0.07	−0.11	−0.48*[b]	−0.08	−0.08	−0.34	−0.13	−0.2	−0.09	−0.38	0.003	−0.09	1	
toluene	0.60**	0.54**	0.05	0.43*	0.52**	0.44*	0.34	0.61**	0.37	0.63**	0.54**	0.59**	0.60**	0.52**	0.62**	0.35	0.65**	−0.1	1

[a] ** Correlation is significant at the 0.01 level (2-tailed).
[b] * Correlation is significant at the 0.05 level.

end-product during the atmospheric oxidation.

3.2.2. PAHs, OPAHs, and n-alkane

The average A/F ratios for the PAHs, OPAHs, and n-alkane group are 6.5 ± 3.7, 17.9 ± 1.2 and 9.6 ± 0.5, respectively. The A/F ratios for the individual PAH (range from 3.4 to 15.8) are much lower than those of OPAHs, representing that the formations of parent PAHs are less than their uptakes in the formations of corresponding OPAHs during the photochemical aging. Besides, the increase of particle number concentration in the chamber could produce a large sink to both freshly emitted gas-phase and particulate-phase PAHs. Consequently, more photochemical oxidations led to the declines of particle-phase parent PAHs. The EF_{aged} of the 16 priority PAHs account for 72.1–77.6% of total quantified PAHs, slightly lower than the EF_{fresh} of 83.2–84.8%, further support their degradations in the stimulated aging process. The total EF_{aged} (59913.8 ± 3286.9 ng kg^{-1}) for Group B2 PAHs is ~4.6 times the EF_{fresh} (13003.5 ± 747.8 ng kg^{-1}). A previous study demonstrated that the particulate PAHs could enhance particle-induced inflammatory in lung tissues (Heinrich et al., 1994).

The ratios of corresponding oxidized PAH (OPAH)/parent-PAH are listed in Table 2 and compared in Fig. 2. Many studies found that the parent-PAHs could be oxidized to form OPAHs during the atmospheric photochemical reactions (Li et al., 2020a, 2020b), and their ratios are often used as indicator for atmospheric aging (Bandowe et al., 2021). In this study, the A/F ratios for the oxidized form (OPAH)/parent PAH of 1, 4-naphthoquinone/naphthalene, 9-fluorenone/fluorene, 1-acenaphthenone/acenaphthene, and 1-acenaphthenone/acenaphthylene are in a range of 16.4–20.9, supporting the elaboration of the oxidations of the parent PAHs in the examinations. OPAHs could actively induce toxicological impacts such as mutagenic, carcinogenic, and cytotoxic effects (Misaki et al., 2016; Wilson et al., 1996; Wincent et al., 2016). The OPAHs can react with DNA, RNA, proteins and lipids under exposure to the organism, resulting in the formation of reactive oxygen species (ROS) and further oxidative damage to the biological molecules (Chung et al., 2006; Gbeddy et al., 2020; Lin et al., 2015). The International Agency for Research on Cancer (IRAC) classifies 9,10-anthraquinone as a possible human carcinogen (Group 2 B) (IARC, 2013). A past study used zebrafish embryos exposure (from 6 to 120 h post fertilization (hpf)) to 38 different OPAHs and the result showed that 1,4-naphthoquinone was the most toxic OPAH, causing 100% mortality at 24 hpf for all concentrations (Knecht et al., 2013). The 1,4-Naphthoquinones may possibly cause oxidative stress in exposed cells (Klotz et al., 2014). A study showed that 9-fluorenone and 1,4-naphthoquinone were the two most dominant compounds in the soils from different types of land at Newcastle in Australia (Idowu et al., 2020).

The A/F ratios for the n-alkane group are in a range of 7.9–10.1, suggest that they are relatively stable during the atmospheric aging process in comparison other chemical groups. Despite their saturated chemical configurations, n-alkanes are considered as low-volatility precursors that are useful to investigate SOA formation from photooxidation and further estimation of the SOA yield (Presto et al., 2010).

3.3. Correlations between degradation of volatile organic compounds (VOCs) and formations of organic acids

Table 3 list the correlations between degradations of VOCs and formations of organic acids during the aging processes (Lyu et al., 2019). Here, the degradation of VOC is defined as the amounts of a representative photochemically-active aromatic (i.e., benzene or toluene) consumed against the formations of organic acids after stimulated atmospheric aging.

Strong positive correlations ($r > 0.6$) are seen between the degradation of toluene and formations of pinonic acid, succinic acid, adipic acid, terephthalic acid, glutaric acid and citramalic acid after the aging process. Sato et al. (2007) demonstrated the photooxidation of toluene could produce different chemical components (e.g., diacids and

oligomers) that consequently lead to the SOA formation in urban atmosphere (Sato et al., 2007). Unsaturated diacids are produced by the photochemical oxidation of aromatic hydrocarbons such as toluene and naphthalene (Kawamura and Ikushima, 1993; Kawamura and Yasui, 2005).

Moderate positive correlations ($r > 0.5$) are also observed between degradation of toluene and the formations of other acids such as isopimaric acid, malonic acid and isophthalic acid. A study demonstrated that bifunctional organic acids could be secondarily produced in the atmosphere by photochemical processes, while a positive relationship ($r = 0.85$) was observed between the concentrations of total diacid compounds and non-methane hydrocarbons (NMHCs) (Kawamura and Yasui, 2005). However, no monocarboxylic acid, and saturated and unsaturated acid show moderate to strong positive correlations with benzene, implying that photo-chemical reactivity of benzene toward the formations of organic acids are much weaker than that of toluene. The above findings warrant further investigation on the photochemical transformation pathways in productions of organic acids, especially the SOA tracers, in urban atmosphere.

4. Conclusions

The characteristics were investigated of primary and secondary emissions from gasoline vehicles. The EF_{fresh} for the dominant component in aromatic acid group is phthalic acid (3.4–92.5 ng kg^{-1}) and probably derived from incomplete combustion products of aromatic hydrocarbons (benzene, toluene and naphthalene) in vehicle engines. Extremely high A/F ratios (>300) under steady state for 2,3-dihydroxy-4-oxopentanoic acid can possibly be related to rapid formation rate of the compounds or decarboxylation process during aging. Distinctive differences were found in the abundances of specific chemical species in gasoline exhaust, but the variations among individual exhaust profiles were large. These variations should be considered when applying specific profiles in receptor modelling or emission inventory development and in estimating the uncertainties associated with the results. Additional studies should focus on quantifying and harmonizing these uncertainties to improve future analyses. The implications of this study are to elucidate the chemical properties of fresh and aged PM emissions from gasoline vehicles. The outcome can further be used for evidence-based policy making.

Author contribution

Ka Hei Lui: Conceptualization, Methodology, Writing – review & editing, Formal analysis, Writing – original draft, Data curation, Investigation, Validation. Yik-Sze Lau: Conceptualization, Writing – original draft, Formal analysis, Software. HonYin Poon: Validation, Investigation. Bruce Organ: Validation, Investigation. Man-Nin Chan: Validation, Investigation. Hai Guo: Project administration, Validation, Resources. Steven Sai Hang Ho: Methodology, Validation, Investigation, Project administration. Kin Fai Ho: Conceptualization, Methodology, Funding acquisition, Project administration, Supervision.

Declaration of competing interest

The authors declare that they have no known competing financial interests or personal relationships that could have appeared to influence the work reported in this paper.

Data availability

Data will be made available on request.

Acknowledgments

This study was supported by the Research Grants Council of the Hong Kong Special Administrative Region China, General Research Fund (Project No. 14205318).

Appendix A. Supplementary data

Supplementary data to this article can be found online at https://doi.org/10.1016/j.chemosphere.2023.138940.

References

Alkidas, A.C.J.E.C., Management, 2007. Combustion advancements in gasoline engines 48, 2751–2761.
Alkurdi, F., Karabet, F., Dimashki, M.J.A.R., 2013. Characterization, concentrations and emission rates of polycyclic aromatic hydrocarbons in the exhaust emissions from in-service vehicles in. Damascus 120, 68–77.
ATSDR, 1995. Toxicological Profile for Polycyclic Aromatic Hydrocarbons (PAHs). http://www.atsdr.cdc.gov/toxprofiles/tp69.pdf.
Baltensperger, U., Dommen, J., Alfarra, M.R., Duplissy, J., Gaeggeler, K., Metzger, A., et al., 2008. Combined determination of the chemical composition and of health effects of secondary organic aerosols. The POLYSOA project 21, 145–154.
Bandowe, B.A.M., Lui, K., Jones, T., BeruBe, K., Adams, R., Niu, X., et al., 2021. The Chemical Composition and Toxicological Effects of Fine Particulate Matter (PM2. 5) Emitted from Different Cooking Styles, vol. 288, 117754.
Bock, N.R., Baum, M.M., Moss, J.A., Castonguay, A.E., Jocic, S., Northrop, W.F.J.F., 2020. Dicarboxylic Acid Emissions from a GDI Engine Equipped with a Catalytic Gasoline Particulate Filter, vol. 275, 117940.
Bond, T.C., Streets, D.G., Yarber, K.F., Nelson, S.M., Woo, J.H., Klimont ZJJoGRA, 2004. A Technology Based Global Inventory of Black and Organic Carbon Emissions from Combustion, vol. 109.
Borrás, E., Tortajada-Genaro, L.A.J.A.E., 2012. Secondary Organic Aerosol Formation from the Photo-Oxidation of Benzene, vol. 47, pp. 154–163.
Boström, C.-E., Gerde, P., Hanberg, A., Jernström, B., Johansson, C., Kyrklund, T., et al., 2002. Cancer Risk Assessment, Indicators, and Guidelines for Polycyclic Aromatic Hydrocarbons in the Ambient Air, vol. 110, pp. 451–488.
Chebbi, A., Carlier, P.J.A.E., 1996. Carboxylic Acids in the Troposphere, Occurrence, Sources, and Sinks: A Review, vol. 30, pp. 4233–4249.
Cheung, K., Ntziachristos, L., Tzamkiozis, T., Schauer, J., Samaras, Z., Moore, K., et al., 2010. Emissions of Particulate Trace Elements, Metals and Organic Species from Gasoline, Diesel, and Biodiesel Passenger Vehicles and Their Relation to Oxidative Potential, vol. 44, pp. 500–513.
Chung, M.Y., Lazaro, R.A., Lim, D., Jackson, J., Lyon, J., Rendulic, D., et al., 2006. Aerosol-borne Quinones and Reactive Oxygen Species Generation by Particulate Matter Extracts, vol. 40, pp. 4880–4886.
Davis, S.C., Williams, S.E., Boundy, R.G., Moore, S., 2015. Vehicle Technologies Market Report. Oak Ridge National Lab.(ORNL), Oak Ridge, TN (United States), 2016.
Fraser, M.P., Cass, G.R., Simoneit Brjes, technology, 1998. Gas-Phase and Particle-phase Organic Compounds Emitted from Motor Vehicle Traffic in a Los Angeles Roadway Tunnel, vol. 32, pp. 2051–2060.
Fraser, M.P., Cass, G.R., Simoneit, B.R.J.A.E., 1999. Particulate Organic Compounds Emitted from Motor Vehicle Exhaust and in the Urban Atmosphere, vol. 33, pp. 2715–2724.
Fujita, E.M., Zielinska, B., Campbell, D.E., Arnott, W.P., Sagebiel, J.C., Mazzoleni, L., et al., 2007. Variations in Speciated Emissions from Spark-Ignition and Compression-Ignition Motor Vehicles in California's South Coast Air Basin, vol. 57, pp. 705–720.
Gbeddy, G., Goonetilleke, A., Ayoko, G.A., Egodawatta, P.J.E.P., 2020. Transformation and Degradation of Polycyclic Aromatic Hydrocarbons (PAHs) in Urban Road Surfaces: Influential Factors, Implications and Recommendations, vol. 257, 113510.
Gentner, D.R., Jathar, S.H., Gordon, T.D., Bahreini, R., Day, D.A., El Haddad, I., et al., 2017. Review of Urban Secondary Organic Aerosol Formation from Gasoline and Diesel Motor Vehicle Emissions, vol. 51, pp. 1074–1093.
Gordon, T., Presto, A., May, A., Nguyen, N., Lipsky, E., Donahue, N., et al., 2014. Secondary Organic Aerosol Formation Exceeds Primary Particulate Matter Emissions for Light-Duty Gasoline Vehicles, vol. 14, pp. 4661–4678.
Grosjean, D., Seinfeld, J.H.J.A.E., 1989. Parameterization of the Formation Potential of Secondary Organic Aerosols, vol. 23, pp. 1733–1747.
Hamilton, J., Lewis, A., Reynolds, J., Carpenter, L., Lubben, A.J.A.C., 2006. Physics. Investigating the Composition of Organic Aerosol Resulting from Cyclohexene Ozonolysis: Low Molecular Weight and Heterogeneous Reaction Products, vol. 6, pp. 4973–4984.
Hatakeyama, S., Tanonaka, T., Weng, J., Bandow, H., Takagi, H., Hjes, Akimoto, et al., 1985. Ozone-cyclohexene Reaction in Air: Quantitative Analysis of Particulate Products and the Reaction Mechanism, vol. 19, pp. 935–942.
Hayes, P.L., Carlton, A.G., Baker, K.R., Ahmadov, R., Washenfelder, R.A., Alvarez, S., et al., 2015. Modeling the Formation and Aging of Secondary Organic Aerosols in Los Angeles during CalNex 2010, vol. 15, pp. 5773–5801.
He, L.-Y., Hu, M., Huang, X.-F., Zhang, Y.-H., Yu, B.-D., Liu, D.-Q.J.C., 2006. Chemical Characterization of Fine Particles from On-Road Vehicles in the Wutong Tunnel in Shenzhen, China, vol. 62, pp. 1565–1573.
Heinrich, U., Roller, M., Fjtl, Pott, 1994. Estimation of a Lifetime Unit Lung Cancer Risk for Benzo (A) Pyrene Based on Tumour Rates in Rats Exposed to Coal Tar/pitch Condensation Aerosol, vol. 72, pp. 155–161.

Herring, C.L., Faiola, C.L., Massoli, P., Sueper, D., Erickson, M.H., McDonald, J.D., et al., 2015. New Methodology for Quantifying Polycyclic Aromatic Hydrocarbons (PAHs) Using High-Resolution Aerosol Mass Spectrometry, vol. 49, pp. 1131–1148.
Hong Kong Transport Department, 2021. The government of the Hong Kong special administrative region. Monthly Traffic and Transport Digest.
Huang, L., Bohac, S.V., Chernyak, S.M., Batterman, S.A.J.W., Air, Pollution, S., 2013. Composition and Integrity of PAHs, Nitro-PAHs, Hopanes, and Steranes in Diesel Exhaust Particulate Matter, vol. 224, pp. 1–14.
IARC, 2010. International agency for Research on cancer, monographs on the evaluation of carcinogenic risk of chemicals to humans. In: Some Non-heterocyclic Polycyclic Aromatic Hydrocarbons and Some Related Exposures. IARC, Lyon.
IARC, 2013. Some chemicals present in industrial and consumer products, food and drinking-water. In: IARC Monographs on the Evaluation of Carcinogenic Risks to Humans (Lyon, France).
Idowu, O., Semple, K.T., Ramadass, K., O'Connor, W., Hansbro, P., PjsotTE, Thavamani, 2020. Analysis of Polycyclic Aromatic Hydrocarbons (PAHs) and Their Polar Derivatives in Soils of an Industrial Heritage City of Australia, vol. 699, 134303.
Jahirul, M.I., Masjuki, H.H., Saidur, R., Kalam, M., Jayed, M., Wazed, M.J.A.T.E., 2010. Comparative Engine Performance and Emission Analysis of CNG and Gasoline in a Retrofitted Car Engine, vol. 30, pp. 2219–2226.
Jimenez, J.L., Canagaratna, M., Donahue, N., Prevot, A., Zhang, Q., Kroll, J.H., et al., 2009. Evolution of Organic Aerosols in the Atmosphere, vol. 326, pp. 1525–1529.
Kawamura, K., Gagosian, R.J.N., 1987. Implications of ω-oxocarboxylic Acids in the Remote Marine Atmosphere for Photo-Oxidation of Unsaturated Fatty Acids, vol. 325, pp. 330–332.
Kawamura, K., Ikushima, K.J.E.S., 1993. Technology. Seasonal Changes in the Distribution of Dicarboxylic Acids in the Urban Atmosphere, vol. 27, pp. 2227–2235.
Kawamura, K., Yasui, O.J.A.E., 2005. Diurnal Changes in the Distribution of Dicarboxylic Acids, Ketocarboxylic Acids and Dicarbonyls in the Urban Tokyo Atmosphere, vol. 39, pp. 1945–1960.
Kawamura, K., Ng, L.L., Kaplan, IRJEs, 1985. Technology. Determination of Organic Acids (C1-C10) in the Atmosphere, Motor Exhausts, and Engine Oils, vol. 19, pp. 1082–1086.
Kawamura, K., Kaplan, 1987. IRJEs Technology. Motor Exhaust Emissions as a Primary Source for Dicarboxylic Acids in Los Angeles Ambient Air, vol. 21, pp. 105–110.
Kawamura, K., Kasukabe, H., Barrie, L.A.J.A.E., 1996. Source and Reaction Pathways of Dicarboxylic Acids, Ketoacids and Dicarbonyls in Arctic Aerosols: One Year of Observations, vol. 30, pp. 1709–1722.
Kawamura, K., Steinberg, S., Kaplan, I.R.J.A.E., 2000. Homologous Series of C1–C10 Monocarboxylic Acids and C1–C6 Carbonyls in Los Angeles Air and Motor Vehicle Exhausts, vol. 34, pp. 4175–4191.
Keywood, M., Kroll, J., Varutbangkul, V., Bahreini, R., Flagan, R., Jjes, Seinfeld, et al., 2004a. Secondary Organic Aerosol Formation from Cyclohexene Ozonolysis: Effect of OH Scavenger and the Role of Radical Chemistry, vol. 38, pp. 3343–3350.
Keywood, M., Varutbangkul, V., Bahreini, R., Flagan, R., Seinfeld Jjes, technology, 2004b. Secondary Organic Aerosol Formation from the Ozonolysis of Cycloalkenes and Related Compounds, vol. 38, pp. 4157–4164.
Kittelson, D., Watts, W., Johnson, J., Schauer, J., Lawson DJJoAS, 2006a. On-road and Laboratory Evaluation of Combustion Aerosols—Part 2:: Summary of Spark Ignition Engine Results, vol. 37, pp. 931–949.
Kittelson, D., Watts, W., Johnson JJJoAS, 2006b. On-road and Laboratory Evaluation of Combustion Aerosols—Part1: Summary of Diesel Engine Results, vol. 37, pp. 913–930.
Kittelson, D., Watts, W., Johnson, J., Thorne, C., Higham, C., Payne, M., et al., 2008. Effect of Fuel and Lube Oil Sulfur on the Performance of a Diesel Exhaust Gas Continuously Regenerating Trap, vol. 42, pp. 9276–9282.
Klotz, L.-O., Hou, X., Jacob, C.J.M., 2014. 1, 4-naphthoquinones: from Oxidative Damage to Cellular and Inter-cellular Signaling, vol. 19, pp. 14902–14918.
Knecht, A.L., Goodale, B.C., Truong, L., Simonich, M.T., Swanson, A.J., Matzke, M.M., et al., 2013. Comparative Developmental Toxicity of Environmentally Relevant Oxygenated PAHs, vol. 271, pp. 266–275.
Kundu, S., Kawamura, K., Andreae, T., Hoffer, A., Andreae, M.J.A.C., 2010. Physics. Molecular Distributions of Dicarboxylic Acids, Ketocarboxylic Acids and α-dicarbonyls in Biomass Burning Aerosols: Implications for Photochemical Production and Degradation in Smoke Layers, vol. 10, pp. 2209–2225.
Lambe, A., Ahern, A., Williams, L., Slowik, J., Wong, J., Abbatt, J., et al., 2011. Characterization of Aerosol Photooxidation Flow Reactors: Heterogeneous Oxidation, Secondary Organic Aerosol Formation and Cloud Condensation Nuclei Activity Measurements, vol. 4, pp. 445–461.
Lau, Y.-S., Chan, M.-N., Poon, H.-Y., Tan, Y., Lee, S.-C., Li, J., et al., 2021. Chemical Composition of Gas and Particle Phase Products of Toluene Photooxidation Reaction under High OH Exposure Condition, vol. 12, p. 915.
Lau, Y.-S., Poon, H.-Y., Organ, B., Chuang, H.-C., Chan, M.-N., Guo, H., et al., 2023. Toxicological Effects of Fresh and Aged Gasoline Exhaust Particles in Hong Kong, vol. 441, 129846.
Li, R., Palm, B.B., Ortega, A.M., Hlywiak, J., Hu, W., Peng, Z., et al., 2015. Modeling the Radical Chemistry in an Oxidation Flow Reactor: Radical Formation and Recycling, Sensitivities, and the OH Exposure Estimation Equation, vol. 119, pp. 4418–4432.
Li, J., Liu, Q., Li, Y., Liu, T., Huang, D., Zheng, J., et al., 2019. Characterization of Aerosol Aging Potentials at Suburban Sites in Northern and Southern China Utilizing a Potential Aerosol Mass (Go: PAM) Reactor and an Aerosol Mass Spectrometer, vol. 124, pp. 5629–5649.
Li, J., Li, J., Wang, G., Zhang, T., Dai, W., Ho, K.F., et al., 2020a. Molecular Characteristics of Organic Compositions in Fresh and Aged Biomass Burning Aerosols, vol. 741, 140247.
Li, J., Zhang, Q., Wang, G., Li, J., Wu, C., Liu, L., et al., 2020b. Optical Properties and Molecular Compositions of Water-Soluble and Water-Insoluble Brown Carbon (BrC) Aerosols in Northwest China, vol. 20, pp. 4889–4904.
Liang, B., Ge, Y., Tan, J., Han, X., Gao, L., Hao, L., et al., 2013. Comparison of PM Emissions from a Gasoline Direct Injected (GDI) Vehicle and a Port Fuel Injected (PFI) Vehicle Measured by Electrical Low Pressure Impactor (ELPI) with Two Fuels: Gasoline and M15 Methanol Gasoline, vol. 57, pp. 22–31.
Lin, Y., Ma, Y., Qiu, X., Li, R., Fang, Y., Wang, J., et al., 2015. Sources, Transformation, and Health Implications of PAHs and Their Nitrated, Hydroxylated, and Oxygenated Derivatives in PM2. 5 in Beijing, vol. 120, pp. 7219–7228.
Lin, Y.-C., Li, Y.-C., Shangdiar, S., Chou, F.-C., Sheu, Y.-T., Cheng, P.-C.J.C., 2019. Assessment of PM2. 5 and PAH Content in PM2. 5 Emitted from Mobile Source Gasoline-Fueled Vehicles in Concomitant with the Vehicle Model and Mileages, vol. 226, pp. 502–508.
Lin, Y.-C., Li, Y.-C., Amesho, K.T., Shangdiar, S., Chou, F.-C., Cheng P-CJSoTTE, 2020. Chemical Characterization of PM2. 5 Emissions and Atmospheric Metallic Element Concentrations in PM2. 5 Emitted from Mobile Source Gasoline-Fueled Vehicles, vol. 739, 139942.
Lough, G.C., Christensen, C.G., Schauer, J.J., Tortorelli, J., Mani, E., Lawson, D.R., et al., 2007. Development of Molecular Marker Source Profiles for Emissions from On-Road Gasoline and Diesel Vehicle Fleets, vol. 57, pp. 1190–1199.
Lu, Q., Zhao, Y., Robinson, A.L.J.A.C., Physics, 2018. Comprehensive Organic Emission Profiles for Gasoline, Diesel, and Gas-Turbine Engines Including Intermediate and Semi-volatile Organic Compound Emissions, vol. 18, pp. 17637–17654.
Luo, Y., Zhu, L., Fang, J., Zhuang, Z., Guan, C., Xia, C., et al., 2015. Size Distribution, Chemical Composition and Oxidation Reactivity of Particulate Matter from Gasoline Direct Injection (GDI) Engine Fueled with Ethanol-Gasoline Fuel, vol. 89, pp. 647–655.
Lyu, X., Wang, N., Guo, H., Xue, L., Jiang, F., Zeren, Y., et al., 2019. Causes of a Continuous Summertime O 3 Pollution Event in Jinan, a Central City in the North China Plain, vol. 19, pp. 3025–3042.
Mao, J., Ren, X., Brune, W.H., Olson, J.R., Crawford, J.H., Fried, A., et al., 2009. Airborne Measurement of OH Reactivity during INTEX-B, vol. 9, pp. 163–173.
Miguel, A.H., Kirchstetter, T.W., Harley, R.A., Hering Svjes, Technology, 1998. On-road Emissions of Particulate Polycyclic Aromatic Hydrocarbons and Black Carbon from Gasoline and Diesel Vehicles, vol. 32, pp. 450–455.
Misaki, K., Takamura-Enya, T., Ogawa, H., Takamori, K., Yanagida, M.J.M., 2016. Tumour-promoting Activity of Polycyclic Aromatic Hydrocarbons and Their Oxygenated or Nitrated Derivatives, vol. 31, pp. 205–213.
MmjjoAS, Maricq, 2007. Chemical Characterization of Particulate Emissions from Diesel Engines: A Review, vol. 38, pp. 1079–1118.
Morino, Y., Li, Y., Fujitani, Y., Sato, K., Inomata, S., Tanabe, K., et al., 2022. Secondary Organic Aerosol Formation from Gasoline and Diesel Vehicle Exhaust under Light and Dark Conditions, vol. 2, pp. 46–64.
Muñoz, M., Haag, R., Honegger, P., Zeyer, K., Mohn, J., Comte, P., et al., 2018. Co-formation and Co-release of Genotoxic PAHs, Alkyl-PAHs and Soot Nanoparticles from Gasoline Direct Injection Vehicles, vol. 178, pp. 242–254.
Myung, C.-L., Choi, K., Kim, J., Lim, Y., Lee, J., Park, S.J.E., 2012. Comparative Study of Regulated and Unregulated Toxic Emissions Characteristics from a Spark Ignition Direct Injection Light-Duty Vehicle Fueled with Gasoline and Liquid Phase LPG (Liquefied Petroleum Gas), vol. 44, pp. 189–196.
Nesamani, Nesamani, 2010. Estimation of Automobile Emissions and Control Strategies in India, vol. 408, pp. 1800–1811.
Nordin, E., Eriksson, A., Roldin, P., Nilsson, P., Carlsson, J., Kajos, M., et al., 2013. Secondary Organic Aerosol Formation from Idling Gasoline Passenger Vehicle Emissions Investigated in a Smog Chamber, vol. 13, pp. 6101–6116.
Pey, J., Querol, X., Ajar, Alastuey, 2009. Variations of Levels and Composition of PM10 and PM2. 5 at an Insular Site in the Western Mediterranean, vol. 94, pp. 285–299.
Platt, S.M., El Haddad, I., Zardini, A.A., Clairotte, M., Astorga, C., Wolf, R., et al., 2013. Secondary Organic Aerosol Formation from Gasoline Vehicle Emissions in a New Mobile Environmental Reaction Chamber, vol. 13, pp. 9141–9158.
Pope III, C.A., Dwjjota, Dockery, association, wm, 2006. Health Effects of Fine Particulate Air Pollution: Lines that Connect, vol. 56, pp. 709–742.
Presto, A.A., Miracolo, M.A., Donahue, N.M., Robinson Aljes, technology, 2010. Secondary Organic Aerosol Formation from High-NO X Photo-Oxidation of Low Volatility Precursors: N-Alkanes, vol. 44, pp. 2029–2034.
Rogge, W.F., Hildemann, L.M., Mazurek, M.A., Cass, G.R., Simoneit Brjes, technology, 1993. Sources of Fine Organic Aerosol. 2. Noncatalyst and Catalyst-Equipped Automobiles and Heavy-Duty Diesel Trucks, vol. 27, pp. 636–651.
Saha, P.K., Khlystov, A., Snyder, M.G., Grieshop, A.P.J.A.E., 2018. Characterization of Air Pollutant Concentrations, Fleet Emission Factors, and Dispersion Near a North Carolina Interstate Freeway across Two Seasons, vol. 177, pp. 143–153.
Sánchez-Ccoyllo, O.R., Ynoue, R.Y., Martins, L.D., Astolfo, R., Miranda, R.M., Freitas, E. D., et al., 2009. Vehicular particulate matter emissions in road tunnels in Sao Paulo. Brazil 149, 241–249.
Sato, K., Hatakeyama, S., Imamura TJTJoPCA, 2007. Secondary Organic Aerosol Formation during the Photooxidation of Toluene: NO X Dependence of Chemical Composition, vol. 111, pp. 9796–9808.
Schauer, J.J., Kleeman, M.J., Cass, G.R., Simoneit Brjes, technology, 2002. Measurement of Emissions from Air Pollution Sources. 5. C1− C32 Organic Compounds from Gasoline-Powered Motor Vehicles, vol. 36, pp. 1169–1180.
Schauer, J., Christensen, C., Kittelson, D., Johnson, J., Watts Wjas, Technology, 2008. Impact of Ambient Temperatures and Driving Conditions on the Chemical Composition of Particulate Matter Emissions from Non-smoking Gasoline-Powered Motor Vehicles, vol. 42, pp. 210–223.

Stocker, T., Qin, D., Plattner, G., Tignor, M., Allen, S., Boschung, J., et al., 2013. The Physical Science Basis. Contribution of Working Group I to the Fifth Assessment Report of the Intergovernmental Panel on Climate Change, vol. 18, pp. 95–123.

Tkacik, D.S., Lambe, A.T., Jathar, S., Li, X., Presto, A.A., Zhao, Y., et al., 2014. Secondary Organic Aerosol Formation from In-Use Motor Vehicle Emissions Using a Potential Aerosol Mass Reactor, vol. 48, pp. 11235–11242.

U.S. Centers for disease control agency for toxic substances and disease registry (ATSDR), 1995. Toxicological Profile for Polycyclic Aromatic Hydrocarbons (PAHs). http://www.atsdr.cdc.gov/toxprofiles/tp69.pdf.

U.S. Department of Energy, Office of Energy Efficiency & Renewable Energy, Vehicle Technologies Office, 2021. Annual Progress Report.

Wang, B., Lau, Y.-S., Huang, Y., Organ, B., Lee, S.-C., Ho, K.-F.J.A.Q., Atmosphere, et al., 2019. Investigation of Factors Affecting the Gaseous and Particulate Matter Emissions from Diesel Vehicles, vol. 12, pp. 1113–1126.

Watne, Å.K., Psichoudaki, M., Ljungstrom, E., Le Breton, M., Hallquist, M., Jerksjo, M., et al., 2018. Fresh and oxidized emissions from in-use transit buses running on diesel. biodiesel, and CNG 52, 7720–7728.

Went, F.W.J.N., 1960. Blue hazes in the atmosphere 187, 641–643.

Wentzell, J.J., Liggio, J., Li, S.-M., Vlasenko, A., Staebler, R., Lu, G., et al., 2013. Measurements of Gas Phase Acids in Diesel Exhaust: a Relevant Source of HNCO?, vol. 47, pp. 7663–7671.

Wilson, A.S., Davis, C.D., Williams, D.P., Buckpitt, A.R., Pirmohamed, M., Park, B.K.J.T., 1996. Characterisation of the Toxic Metabolite (S) of Naphthalene, vol. 114, pp. 233–242.

Wincent, E., Le Bihanic, F., Kjtr, Dreij, 2016. Induction and Inhibition of Human Cytochrome P4501 by Oxygenated Polycyclic Aromatic Hydrocarbons, vol. 5, pp. 788–799.

Zhang, Q., Jimenez, J.L., Canagaratna, M., Allan, J.D., Coe, H., Ulbrich, I., et al., 2007. Ubiquity and Dominance of Oxygenated Species in Organic Aerosols in Anthropogenically-influenced Northern Hemisphere Midlatitudes, vol. 34.

Zhang, Y., Deng, W., Hu, Q., Wu, Z., Yang, W., Zhang, H., et al., 2020a. Comparison between Idling and Cruising Gasoline Vehicles in Primary Emissions and Secondary Organic Aerosol Formation during Photochemical Ageing, vol. 722, 137934.

Zhang, Z., Zhu, W., Hu, M., Wang, H., Chen, Z., Shen, R., et al., 2020b. Secondary Organic Aerosol from Typical Chinese Domestic Cooking Emissions, vol. 8, pp. 24–31.

Zhao, Y., Saleh, R., Saliba, G., Presto, A.A., Gordon, T.D., Drozd, G.T., et al., 2017. Reducing Secondary Organic Aerosol Formation from Gasoline Vehicle Exhaust, vol. 114, pp. 6984–6989.

Zhao, Y., Lambe, A.T., Saleh, R., Saliba, G., Robinson Aljes, technology, 2018. Secondary Organic Aerosol Production from Gasoline Vehicle Exhaust: Effects of Engine Technology, Cold Start, and Emission Certification Standard, vol. 52, pp. 1253–1261.

Zielinska, B., Sagebiel, J., McDonald, J.D., Whitney, K., , Lawson DRJJotA, Association, W.M., 2004. Emission Rates and Comparative Chemical Composition from Selected In-Use Diesel and Gasoline-Fueled Vehicles, vol. 54, pp. 1138–1150.

Zimmerman, N., Wang, J.M., Jeong, C.-H., Ramos, M., Hilker, N., Healy, R.M., et al., 2016. Field Measurements of Gasoline Direct Injection Emission Factors: Spatial and Seasonal Variability, vol. 50, pp. 2035–2043.